

## Adsorption of o-hydroxybenzoic acid on polymers in supercritical carbon dioxide medium: experimental and modeling

S. Diankov<sup>1\*</sup>, P. Subra-Paternault<sup>2</sup>, I. Hinkov<sup>1</sup>, I. Pentchev<sup>1</sup>

<sup>1</sup> University of Chemical Technology and Metallurgy – Sofia, Bulgaria

<sup>2</sup> Université de Bordeaux, France

Received: October 17, 2010; accepted: April 26, 2011

In this work we present an experimental set-up used for semi-continuous impregnation per adsorption process of polymers with an organic model component (o-hydroxybenzoic acid – o-HBA) using supercritical CO<sub>2</sub> as solvent and impregnating medium. The aim is to study the effect of the supercritical solvent flow-rate, the pressure and the polymer support on the breakthrough volume and the adsorbed quantity. The regular sampling of the supercritical phase is analyzed by High Performance Liquid Chromatography. It is found that the uptake increases with the pressure and decreases with the supercritical solvent flow-rate. In addition, a 1D model with local equilibrium is developed. The model fits well to the breakthrough curves. The numerically obtained values are in good agreement with the experimental results.

**Key words:** supercritical carbon dioxide, impregnation, modeling.

### INTRODUCTION

During the past several decades, processes carried out in supercritical (SC) media have been widely applied in the chemistry and processing of polymers. The impregnation assisted by SC solvents reveals certain advantages compared to traditional methods. The potential of supercritical fluids (SCF) to replace some traditional toxic solvents results from their specific properties: capacity to dissolve solids, related to their high density; transport capacity, related to the viscosity and diffusion coefficient inciting their excellent penetrability. Therefore, various possibilities for controlled drug delivery systems fabrication were investigated [1-5]. Thus, the amount of the impregnated substance is very important for the posterior application of the product. Especially in pharmaceuticals it is required that the product would not be contaminated with residual solvent, hence the interest in using SCF as impregnation media.

### EXPERIMENTAL

The experimental setup is presented schematically in Figure 1. It includes three modules: a dissolution module with a reservoir, where the solute is dissolved in supercritical CO<sub>2</sub>; an impregnation module with a polymer charged

column and a sampling module consisting of a sampling loop. Experiments were performed in two sequential steps: dissolution of the o-HBA in the supercritical CO<sub>2</sub> and impregnation of the solute in the polymer. The inlet side of the column (Top Industries, 10 cm<sup>3</sup>) was filled to 60% of the total volume with inert packing (glass beads, 2 mm) to ensure better flow distribution before the adsorption section. The adsorption section was filled with a mixture of polymer and glass beads of the same size as the polymer (125 to 250 μm). The method is described in detail in our previous work [6]. Two polymers were used in this study: polymethyl methacrylate - PMMA (Plexidon Spain, 95%) and adsorbent resin Amberlite XAD-7 - AmbXAD7 (Fluka), porosity 55% vol., density between 1.06 and 1.08 g/cm<sup>3</sup>, specific surface superior to 400 m<sup>2</sup>/g and average pore diameter of 80 Å.

### EXPERIMENTAL RESULTS AND DISCUSSION

The reliability of the method was demonstrated by three experiments, using 1 gram of PMMA under the same operating conditions. The CO<sub>2</sub> flow-rate was fixed at 0.67 cm<sup>3</sup>/min; the temperature inside the furnace at 40°C and the pressure at 20 MPa. The obtained breakthrough curves are compared in Figure 2. All experimental curves show identical breakthrough time and similar behavior. The average concentration at the plateau (0.175; 0.148 and 0.163 mg<sub>(o-HBA)</sub>/g<sub>(CO<sub>2</sub>)</sub> for

\* To whom all correspondence should be sent:  
e-mail: sdiankov@yahoo.com

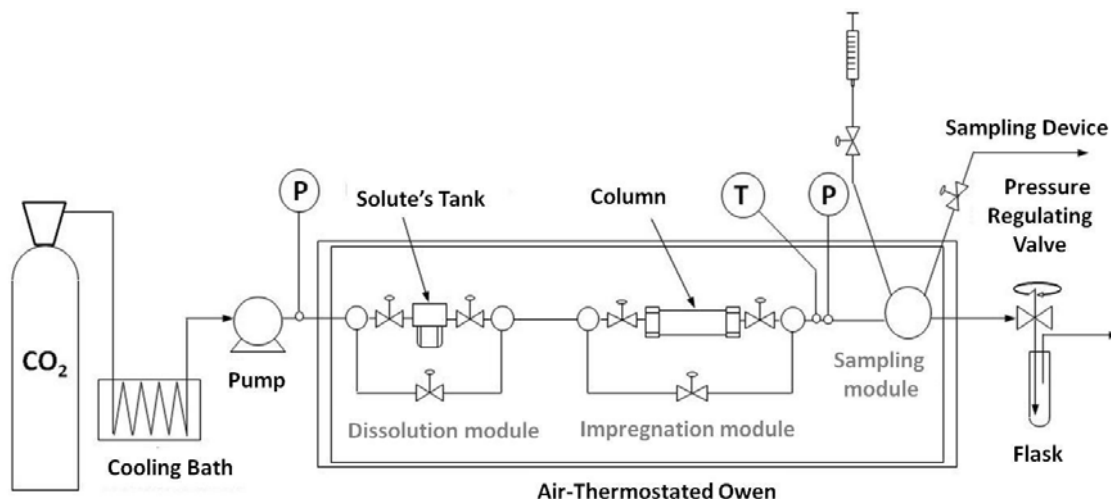


Fig. 1. Experimental setup.

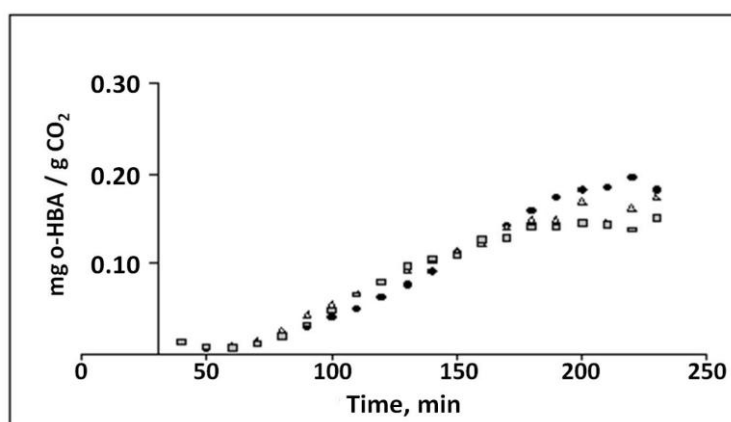


Fig. 2. Three breakthrough curves obtained using  $\text{CO}_2$  flow rate =  $0.67 \text{ cm}^3/\text{min}$ ; temperature =  $40^\circ\text{C}$  and pressure = 20 MPa.

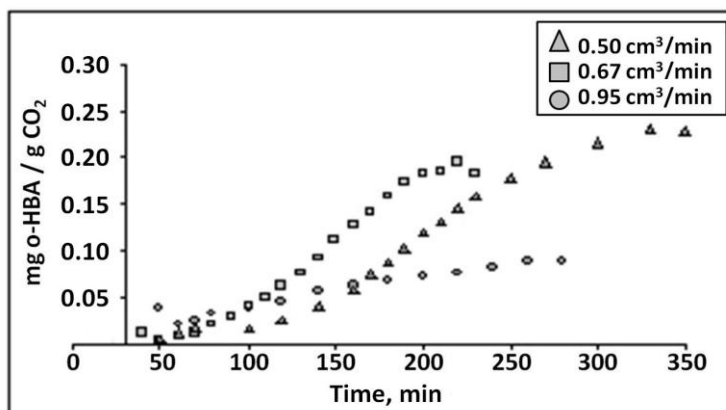


Fig. 3. Breakthrough curves obtained for three  $\text{CO}_2$  flow rates; temperature =  $40^\circ\text{C}$  and pressure = 20 MPa. The polymer is PMMA.

the three experiments, respectively) was determined as an average of four replicates analysis. The maximum uncertainty is about 17%.

The impregnated amount in the polymer was determined by High Performance Liquid Chromatography (HPLC) analysis. Once the

experiment has finished, the polymer support was mixed with methanol in a stirred vessel. Using the calibration curves, we determined the mass of impregnated substance per mass of polymer. These values were then corrected by the non-impregnated quantity of *o*-HBA dissolved in the  $\text{CO}_2$  and

trapped in the column at the end of the experiment. This quantity  $Q$  in  $mg_{(o-HBA)}$  was calculated by the following equation:

$$Q = V_{col} \cdot \varepsilon \cdot \rho \cdot C_{feed}$$

where  $V_{col}$  is the column volume in  $cm^3$ ;  $\varepsilon$  is the ratio of the void volume and the total volume of the column;  $\rho$  is the  $CO_2$  density in  $g/cm^3$  and  $C_{feed}$  is the feed concentration in  $mg_{(o-HBA)}/g_{(CO_2)}$ .

#### Flow-rate influence study

In order to study the influence of  $CO_2$  flow-rate on the impregnated amount we performed three experiments using 0.50; 0.67 and 0.95  $cm^3/min$ . The other operating parameters were fixed: the temperature at  $40^\circ C$  and the pressure at 20 MPa. The support used for this study was PMMA. The breakthrough curves are presented in Figure 3. The supercritical  $CO_2$  flow-rate, the concentrations at the plateau and the impregnated quantities are summarized in Table 1.

The curves obtained using 0.50 and 0.67  $cm^3/min$  flow-rates show a similar trend, however, the breakthrough time (120 and 70 min respectively) and the concentrations at the plateau are different. Increasing the flow-rate to 0.95  $cm^3/min$  leads to significant change in the curve shape. The time necessary to reach the concentration at the plateau is 220 min. The plateau concentration and the impregnated amount decrease

upon increasing the flow-rate. From these results we can conclude that the impregnated amount increases proportionally with the feed concentration of the solute. These results confirm our previous observations [7]. Increasing the solvent flow-rate results in decrease of the residence time in the tank. Thus, a lower amount of dissolved substance is impregnated. Hence, in order to increase the impregnated amount in the polymer, it is necessary to use lower flow-rates.

#### Pressure influence study

In order to study the pressure influence on the impregnated amount, we performed three experiments at 12, 16 and 20 MPa. The  $CO_2$  liquid flow-rate was fixed at 0.5  $cm^3/min$  and the temperature at  $40^\circ C$ . The used support was PMMA. The obtained breakthrough curves are presented in Figure 4. As observed, the curves show similar trend. The breakthrough time remains the same.

However, the time necessary to reach the concentration at the plateau increases upon increasing the pressure. The density of the supercritical  $CO_2$  also increases. This enhances the solvent power and the capacity to dissolve more substances. We should take into consideration that the flow-rate of supercritical solvent containing the solute flow decreases, increasing the pressure.

**Table 1.** : Flow rate influence. Experimental data.

CO <sub>2</sub> flow rate, $cm^3/min$		Concentration at the plateau, $mg_{(o-HBA)}/g_{(CO_2)}$	Impregnated Amount $mg_{(o-HBA)}/g_{(PMMA)}$
Liquid	Supercritical		
0.50	0.59	0.23	16.4
0.67	0.80	0.18	7.0
0.95	1.14	0.09	4.2

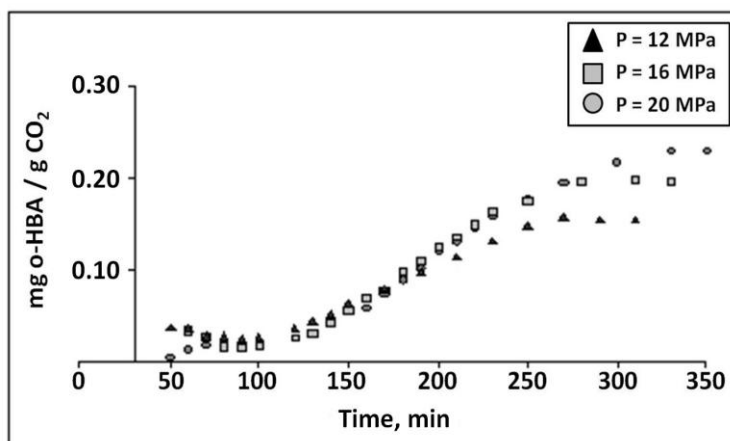


**Fig. 4.** Breakthrough curves at three pressures; Liquid  $CO_2$  flow rate = 0.5  $cm^3/min$ ; temperature =  $40^\circ C$  and pressure P = 20 MPa. The polymer is PMMA.

**Table 2.** Pressure influence study. Experimental data.

P	Liquid CO <sub>2</sub> density	Supercritical CO <sub>2</sub> density	Supercritical CO <sub>2</sub> flow rate	Concentration at the plateau	Impregnated Amount
MPa	g/cm <sup>3</sup>	g/cm <sup>3</sup>	cm <sup>3</sup> /min	mg <sub>(<i>o</i>-HBA)</sub> /g <sub>(CO<sub>2</sub>)</sub>	mg <sub>(<i>o</i>-HBA)</sub> /g <sub>(PMMA)</sub>
12	0.975	0.681	0.79	0.16	7.5
16	0.991	0.792	0.64	0.20	12.7
20	1.013	0.857	0.59	0.23	16.4

**Table 3.** Support influence. Experimental data.

Pressure MPa	Support	Supercritical CO <sub>2</sub> flow rate cm <sup>3</sup> /min	Concentration at the plateau mg <sub>(<i>o</i>-HBA)</sub> /g <sub>(CO<sub>2</sub>)</sub>	Impregnated quantity mg <sub>(<i>o</i>-HBA)</sub> /g <sub>Support</sub>
16	PMMA	0.64	0.20	12.7
16	AmbXAD7	0.64	0.20	79.6
20	PMMA	0.59	0.23	16.4
20	AmbXAD7	0.59	0.23	90.0

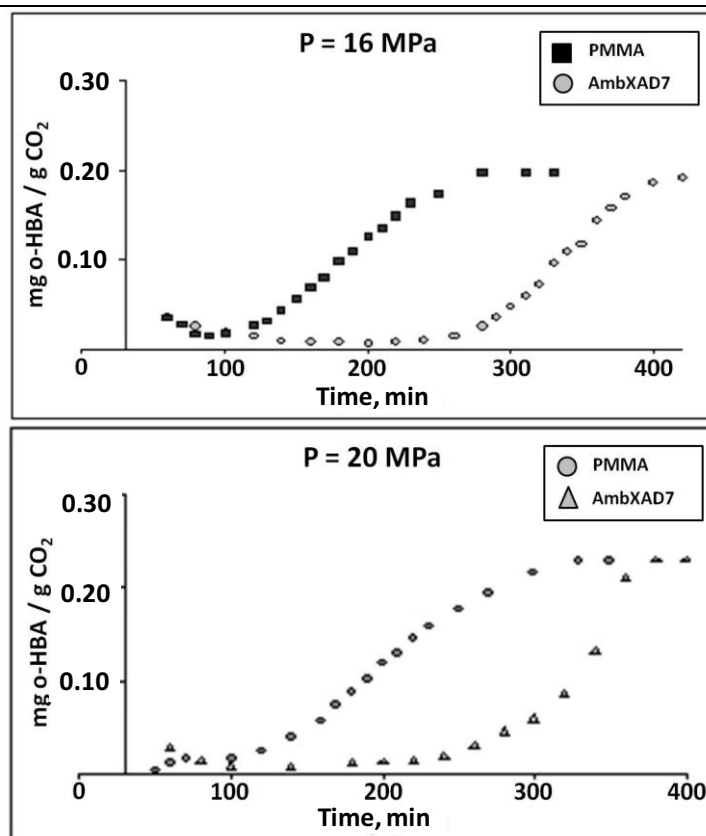


**Fig. 5.** Breakthrough curves obtained at 16 MPa and 20 MPa, Liquid CO<sub>2</sub> flow rate = 0.5 cm<sup>3</sup>/min and Temperature = 40°C.

Therefore the residence time in the solute's tank and the column increases. Both effects contribute to higher feed concentration at higher pressure. The experimental data for CO<sub>2</sub> density, flow-rates, concentrations at the plateau and impregnated amount are summarized in Table 2.

#### Support influence study

For this study we used two polymeric supports: PMMA and AmbXAD7, described above. The operating conditions were: CO<sub>2</sub> liquid flow-rate = 0.5 cm<sup>3</sup>/min, temperature = 40°C, polymer quantity = 1 gram PMMA or 0.5 gram AmbXAD7. The breakthrough curves obtained at two pressures 16

MPa and 20 MPa are plotted on Figure 5. The experimental data are summarized in Table 3. At 16 MPa the breakthrough time for AmbXAD7 is about three times superior (230-250 min), compared to PMMA (70-90 min). For both experiments, the concentrations at the plateau are identical. Therefore, the adsorbed amount on the AmbXAD7 is considerably higher than on the PMMA. These results show the effect of the porosity and the surface area on the impregnated amount. Therefore, we assume that the polymer porosity does not influence the velocity profile inside the column. At a higher pressure (20 MPa), the breakthrough time for AmbXAD7 is 190-210 min. However, it remains the same for the PMMA. The breakthrough curves and the quantities adsorbed are different, probably because at 20 MPa and 40°C in supercritical CO<sub>2</sub>, the PMMA swells and changes its structure.

### MODELING

One-dimensional model (1D) with a basic assumption of local equilibrium was developed in this study. The described experimental process is isothermal and the temperature profile would not influence the equilibrium, respectively the concentration profile. Therefore if the variation of the concentration in radial direction is significant, it will be due to the hydrodynamic factors. The bed porosity fluctuations in a small restricted area close to the wall provoke velocity fluctuations. However, they do not affect the overall concentration profile. Experimental observations [7] show a structure modification (swelling) of the polymer during the contact with SC-CO<sub>2</sub>. Initially the CO<sub>2</sub> molecules are adsorbed in the polymer volume and this allows posterior penetration and adsorption of dissolved compound. For impregnation processes in SC medium, other authors obtain good results assuming that the polymer loses its porosity. They describe the process as a flow through a flat surface [1]. Based on these assumptions, the equation for the mass transfer through the fixed polymer bed is:

$$\varepsilon \frac{\partial C}{\partial t} + \varepsilon \cdot w_z \frac{\partial C}{\partial z} = \varepsilon \cdot D_{ax} \frac{\partial^2 C}{\partial z^2} - (1 - \varepsilon) \frac{\partial q^*}{\partial t} \quad (1)$$

where  $C$  is the concentration in the SC phase and the local equilibrium  $q^* = f(C)$  is described using the Toth relationship:

$$q^* = q_m \frac{b \cdot C}{\left[1 + (b \cdot C)^\theta\right]^{\frac{1}{\theta}}} \quad (2)$$

As boundary conditions we assume equality of the mass flow through the interface and flat concentration profile:

$$D_{ax} \frac{\partial C}{\partial z} \Big|_{z=0} = w_z (C|_{z=0} - C_{feed}) \quad (3)$$

$$\frac{\partial C}{\partial t} \Big|_{z=L} = 0 \quad (4)$$

The initial conditions are:

at  $t = 0 \rightarrow C = 0$  for  $z > 0$

at  $z = 0 \rightarrow C = C_{feed}$  for each  $t$ .

where  $\varepsilon$  is the bed porosity.

When the particle dimension *versus* column diameter ratio is smaller than 0.05 and the number of particle layers in the bed in axial direction is higher than 30, an octahedral arrangement with maximal density of 0.74 could be expected [8]. We estimate a value about 10% greater than the minimal bed porosity:  $\varepsilon = 0.3$ .

$W_z$  is the flow velocity. The flow velocity through the porous bed  $W_z = 2.77 \times 10^{-4}$  m/s corresponds to 0.5 ml/min experimental flow-rate.

$D_{ax}$  is the axial dispersion coefficient. The relationships proposed by some authors [9-13] cannot be directly applied for our study. Therefore, we determined the axial dispersion coefficient using a breakthrough curve obtained without polymeric support. The pattern and the shape of this curve depend only on the axial dispersion and the dead volume of the column. Then, we calculated the breakthrough curves assuming a linear equilibrium, imposing the linear equilibrium factor equal to zero (no adsorption). Thus we obtained the commonly used model for dispersion in fixed bed [11]. We studied the breakthrough curve response in function of the  $D_{ax}$ , all other parameters being already fixed. The best correlation with the experimental data was obtained for  $D_{ax} = 1.6 \times 10^{-6}$  m<sup>2</sup>/s. This value is further used in our numerical simulations.

$q_m$  is the maximum substance load and  $C_{feed}$  – the feed concentration. These values, experimentally obtained for three pressures (12 MPa, 16 MPa and 20 MPa), are presented in Table 4.

**Table 4:** Feed concentration and maximal substance load.

	12 MPa	16 MPa	20 MPa
$C_{feed}$ , mg <sub>(o-HBA)</sub> /g <sub>(CO2)</sub>	0.156	0.198	0.230
$q_m$ , mg <sub>(o-HBA)</sub> /g <sub>(PMMA)</sub>	28.12	28.26	20.66

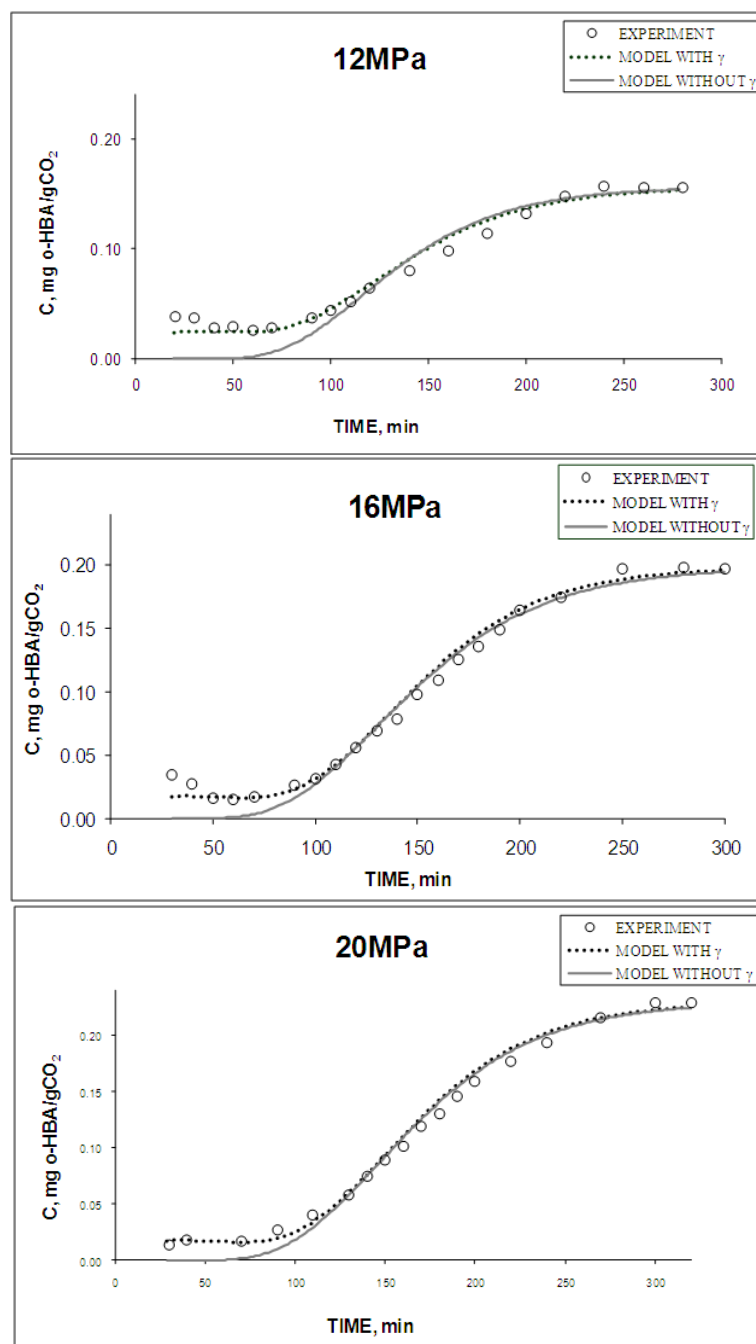


Fig. 6. Comparison of experimental and numerical data.

$b$  and  $\theta$  are the adsorption parameters. The numerical method was initially tested assuming linear equilibrium:  $q_{ads} = k C$ . The parameter  $k$  was adjusted in order to find the best correlation between numerical and experimental data. Next, we introduced the Toth relationship (2) in the equilibrium term. The parameters of the Toth equation were determined in our previous study [7]. However, the kinetic study conditions are different from the equilibrium ones, particularly the two parameters  $b$  and  $\theta$  contribute directly to the

impregnated quantity. For that reason, we considered both parameters adjustable.

For a cylindrical column with fixed bed, the free volume close to the wall is greater than in the centre of the bed. It decreases until stabilization around an average value. That provokes higher velocity of the flow at the wall proximity [14, 15, 16]. The velocity profile strongly depends on the Reynolds number ( $Re$ ). For  $Re > 100$  the fluctuations of the flow profile could be neglected. The percentage of the bypass flow close to the wall is proportional to  $Re$  and the ratio between column and particle diameter ( $D_{col}/d_{part}$ ) and passes through

$$\begin{aligned} & \varepsilon \frac{C_i^{j+1} - C_i^j}{\tau} + \frac{\varepsilon \cdot w_z \cdot \sigma}{h} (C_{i+1}^{j+1} - C_i^{j+1}) + \frac{\varepsilon \cdot w_z \cdot (1 - \sigma)}{h} (C_{i+1}^j - C_i^j) = \\ & = \frac{\varepsilon \cdot D_{ax} \cdot \sigma}{h^2} (C_{i+1}^{j+1} - 2 \cdot C_i^{j+1} + C_{i-1}^{j+1}) + \frac{\varepsilon \cdot D_{ax} \cdot (1 - \sigma)}{h^2} (C_{i+1}^j - 2 \cdot C_i^j + C_{i-1}^j) - (1 - \varepsilon) \frac{\partial q^*}{\partial t} \end{aligned}$$

**Table 5:** Experimental and numerical data for the load.

		Load, $mg_{(o-HBA)}/g_{(PMMA)}$		
		12MPa	16MPa	20MPa
Experimental		7.5	12.7	16.4
Numerical	with $\gamma$	7.4	10.9	16.2
	without $\gamma$	7.9	11.5	16.7

a maximum at  $D_{col}/d_{part} = 10$  [16]. For this study, the  $Re$  number varies from 0.25 to 1.12. At the entry of the column  $D_{col}/d_{part} \approx 5.5$  and the velocity profile is expected to be dispersed. Inside the column  $D_{col}/d_{part} \approx 45$ . Thus, the bypass flow can be neglected and the velocity profile is considered relatively uniform. For reasons of simplicity, we accepted a quasi-uniform profile for the whole column section. Similar hypothesis was proposed by Chern and Chien [17].

The differential equations of the model were approximated by expressing them in finite difference form [18-20]. We used Crank-Nikolson full implicit symmetric scheme with weight coefficient  $\sigma=0.5$ :

Here  $\tau$  and  $h$  are the time and space steps, respectively.

The experimental and numerical results are compared in Figure 6. We found that the model fits well to the experimental data: breakthrough time, slope and plateau concentration. We observed a small divergence in the initial parts of the curves. We supposed that the residence time in the mass transfer zone and the adsorption capacity of PMMA are not sufficient and small quantity of non adsorbed o-HBA remains in the outlet flow ( $\bar{C}_{nonads}$ ). Therefore, we introduced a correction function  $\gamma$  in the equilibrium term:

$$\gamma(t) = \frac{\bar{C}_{nonads}}{\tau^{2.3}}, \text{ using the following boundary}$$

condition:

$\gamma|_{t=0} = \bar{C}_{nonads}$  - in the initial moment the correction function is equal to the average of the experimentally measured concentration in the initial period, and decreases rapidly with the time. This function was adjusted so that its contribution becomes negligible before the breakthrough time.

In order to calculate the impregnated amount we first determined the total amount of substance entering in the column. Then Simpson's method

was used to calculate the surface area below the breakthrough curve. That corresponds to the amount of non adsorbed substance. The difference between these values is the impregnated substance in the PMMA. The calculated loads were compared to the experimental ones in Table 5. Both numerical values (with and without using the correction function  $\gamma$ ) are in good agreement with the experimentally determined quantities.

## CONCLUSIONS

Our experimental study shows the effect of three operating parameters both on the dissolving and impregnation process in supercritical  $CO_2$ . It was found that lower flow-rates allow increasing of the impregnated amount in the polymer support. Higher pressures lead to increase the time necessary to reach the concentration at the plateau. Finally, we found that the impregnated amount on a porous support is considerably higher, compared to a non porous polymer. A 1D model with a basic assumption of local equilibrium was developed in order to describe and understand the process kinetics. The model fits well to the experimental results – breakthrough curves and total impregnated amount.

## REFERENCES

1. O. Guney, A. Akgerman, *AIChE J.*, **48**, 856 (2002).
2. C. Domingo, A. Fanovich, J. Fraile, G. Abraham, J. San Roman, P. Subra, in: *Proc. 8th Meeting on Supercritical Fluids*, **2**, 799 (2002).
3. A. Fanovich, C. Elvira, M. Fernandes, J. San Roman, J. Fraile, C. Domingo, *Chem. Eng. Transactions*, **3**, 551 (2003).
4. C. Magnan, C. Bazan, F. Charbit, J. Joachim, G. Charbit, in: *High Pressure Chemical Engineering*, Ph. Rudolf von Rohr, Ch. Trepp (eds), 1996, p. 509.
5. P.B. Webb, P.C. Marr, A.G. Parsons, H.S. Gidda, S.M. Howdle, *Pure Appl. Chem.*, **72**, 1347 (2004).
6. S. Diankov, P. Subra, I. Pentchev, *Journal of the UCTM*, **37**, 51 (2002).

7. S. Diankov, D. Barth, P. Subra, in: *Proc. 6th International Symposium on Supercritical Fluids*, April 2003, p. 1599.
8. M.A. Goldshtik, *Transfer Processes in Granular Layer*, (in Russian), Acad. Sci. U.S.S.R., Novosibirsk, 1984.
9. D.J. Gunn, *Chem. Eng. Sci.*, **42**, 363 (1987).
10. T. Funazukuri, C. Kong, S. Kagei, *J. Supercrit. Fluids*, **13**, 169 (1998).
11. D. Yu, K. Jackson, T.C. Harmon, *Chem. Eng. Sci.*, **54**, 357 (1999).
12. C-S. Tan, D.C. Liou, *Ind. Eng. Chem. Res.*, **28**, 1246 (1989).
13. S.M. Ghoreishi, A. Akgerman, *Sep. and Pur. Techn.*, **39**, 39 (2004).
14. D. Vortmeyer, K. *Chem. Eng. Sci.*, **40**, 2135 (1985).
15. D. Vortmeyer, R.P. Winter, *Chemical Reaction Engineering*, **196**, 49 (1982).
16. D. Vortmeyer, J. Schuster, *Chem. Eng. Sci.*, **38**, 1691 (1983).
17. J-M. Chern, Y-W. Chien, *Ind. Eng. Chem. Res.*, **40**, 3775 (2001).
18. B.M. Berkovskii, E.F. Nogotov, "*Raznostnie Metodi Issledovania Zadatch Teploobmena*", (in Russian), Nauka i Tehnika, Minsk, 1976, pp. 46-49.
19. E.F. Nogotov, B.M. Berkovskii, W.J. Minkowycz, "*Application of Numerical Heat Transfer*", McGraw-Hill Book Comp., 1978.
20. A.A. Samarski, *Teoria Raznosnih Shem* (in Russian), Nauka, Moskva, 1983, pp.30-35 & 256-260.

## АДСОРБЦИЯ НА О-ХИДРОБЕНЗОЕВА КИСЕЛИНА ВЪРХУ ПОЛИМЕРИ В СРЕДА НА СВРЪХКРИТИЧЕН ВЪГЛЕРОДЕН ДИОКСИД: ЕКСПЕРИМЕНТ И МОДЕЛИРАНЕ

С. Дянков<sup>1\*</sup>, П. Сьубра-Патерно<sup>2</sup>, И. Хинков<sup>1</sup>, И. Пенчев<sup>1</sup>

<sup>1</sup> Химико-технологичен и металургичен университет - София

<sup>2</sup> Университет Бордо, Франция

Постъпила на 17 октомври, 2010 г.; приета на 26 април 2011 г.

(Резюме)

В настоящата работа е представена експериментална инсталация за импрегниране на моделно органично съединение (о-хидробензоева киселина) върху полимери чрез адсорбция в полунепрекъснат режим. Като разтворител и среда за провеждане на процеса е използван свръхкритичен CO<sub>2</sub>. Целта е да се изследва влиянието на дебита на свръхкритичния разтворител, на налягането, както и на полимерната подложка върху проскочните криви и адсорбираното количество. Пробите от свръхкритичната фаза са анализирани чрез Високоэффективна Течна Хроматография. Установено е, че адсорбираното количество нараства при повишаване на налягането и намалява при увеличаването на дебита на свръхкритичния разтворител. Разработен е 1D математичен модел с локално равновесие, който добре описва проскочните криви. Числено получените стойности показват добро съответствие с експерименталните резултати.